**Article ID:** 1003 - 6326(2005)05 - 1055 - 07

# Dynamic recrystallization behavior of AZ61 magnesium alloy①

ZHOU Hai-tao(周海涛)[1], YAN An-qing(严安庆)[2], LIU Chu-ming(刘楚明)[1]
(1. School of Materials Science and Engineering, Central South University, Changsha 410083, China;
2. Institute of Yichang Measurement Technology, Yichang 443003, China)

**Abstract:** An AZ61 alloy was subjected to hot compression at temperatures ranging from 523 K to 673 K, with strain rates of 0.001 - 1 $s^{-1}$. Flow softening occurs at all temperatures and strain rates. There are peak and plateau stresses on flow curves. The initiation and evolution of dynamic recrystallization(DRX) were studied by the flow softening mechanism based on the flow curves and microstructural observations. A linear relationship was established between the logarithmic value of the critical strain for DRX initiation($\ln \varepsilon_c$) and the logarithmic value of the Zener-Hollomon parameter ($\ln Z$). The volume fraction of DRX grain ($\varphi_d$) is formulated as a function of the process parameters including strain rate, temperature, and strain. The calculated values of $\varphi_d$ agree well with the values extracted from the flow curves. The size of DRX grain($d$) was also formulated as a function of the Zener-Hollomon parameter. This study suggests that DRX behavior of AZ61 can be predicated from plastic process parameters.

**Key words:** AZ61 magnesium alloy; dynamic recrystallization; critical strain; flow softening
**CLC number:** TG 376 **Document code:** A

## 1 INTRODUCTION

Magnesium alloys are the lightest metallic structural materials that are attracting more research interest because they have some specific properties like low density, good damping characteristics and stable machinability. However, magnesium alloys have poor formability and limited ductility at room temperature due to the intrinsic characteristics of HCP structure[1-4]. Since non-basal slip systems can be activated at high temperatures (higher than the recrystallization temperature), hot deformation processes have been frequently proposed for magnesium alloys[5]. During hot deformation, some metallurgical phenomena such as work hardening(WH), dynamic recovery (DRV) and dynamic recrystallization(DRX) may occur simultaneously[6, 7], resulting in grain refinement and reduction of deformation resistance. For magnesium alloys, due to their lower stacking fault energy (60 - 78 kJ/mol), DRX predominates during hot deformation (e.g. above 513 K)[8]. Based on the study of recrystallization behaviors of Mg-0.8%Al at a temperature range from 423 K to 523 K, Ion et al[9] suggested that the strain is preferentially located in the vicinity of initial grain boundaries below 603 K, and it was suggested that new grains form at some severely rotated sites (so-called "rotation recrystallization"). Tan et al[10] studied the DRX behaviors of AZ31 alloy and proposed that grain refinement can be attributed to the continuous DRX process that was caused by the progressive formation of grain boundary disorientation and the change of low angle grain boundaries into high angle grain boundaries. Galiyev et al[11] studied the relationship between DRX and deformation mechanism. However, most of these studies are concentrated on microstructure evolution, deformation mechanism or superplasticity. Only few reports are available about the conditions (e.g. critical strain) for DRX initiation, nor has the relationship between processing variables and final microstructures been thoroughly explored.

In the present study, we conducted hot deformation experiments on the AZ61 alloy and recorded the flow stress curves. Typical characteristics of the flow stress curves, i.e. the critical strain ($\varepsilon_c$), the peak strain ($\varepsilon_p$), the strain of maximum softening rate ($\varepsilon_m$) for DRX initiation are evaluated. Then, these parameters are formulated as functions of the Zener-Hollomon parameter with which the volume fraction of DRX can be predicated.

## 2 EXPERIMENTAL

An AZ61 alloy with chemical compositions of Mg-5.8Al-1.0Zn1.0-0.18Mn-0.003Cu (mass fraction, %) was made by chill casting. The ingots were solutionized at 673 K for 15 h. Cylindrical specimens of $d$10 mm × 15 mm were cut out from these ingots.

① **Received date:** 2004 - 12 - 17; **Accepted date:** 2005 - 05 - 09
**Correspondence:** ZHOU Hai-tao, Professor, PhD; Tel: +86-731-8830257; E-mail: htzhou@mail.csu.edu.cn

Hot compression was performed on a Gleeble 1500 machine. Prior to hot compression, the specimens were heated to the deformation temperature in 5 min. The deformation temperature was measured by thermocouples welded onto the center of a specimen surface. The deformation strain, temperature and strain rate were automatically controlled and recorded. Compression was conducted in a temperature ranging from 523 K to 673 K. The strain rates were varied from 0.001 $s^{-1}$ to 1 $s^{-1}$. The total true strain was 1 in all experiments. After hot compression, the specimens were water-quenched. Samples for microstructure observations were cut from compressed specimens along the sections parallel to the compression axis. Grain sizes were determined by the linear intercept method.

## 3 RESULTS AND DISCUSSION

### 3.1 Analyses of flow curves

Fig. 1 shows the stress—strain curves of the AZ61 alloy under different deformation conditions. The general characteristics of the flow stress curves are similar under all deformation conditions. The flow stress increases to a peak (initial strain hardening) and then decreases to a steady state.

Generally, such flow stress behaviors are typical characteristics of hot working that is accompanied by DRX[12, 13], which can be described by the thermally activated stored energy developed during deformation controlled softening mechanisms[11]. With decreasing strain rate or increasing temperature, the strain hardening effect becomes weaken, while the degree of strain softening becomes notable (e.g. 673 K). As a result, the peak stress varies according to processing parameters, so does the peak strain. Under a constant strain rate, the peak stress and the peak strain increase with decreasing temperature. Under the same temperature, the peak stress and the peak strain increases with increasing strain rate. Thus, it can generally be concluded that DRX is responsible for the high temperature deformation mechanism of AZ61 alloy and can be confirmed by comparison of microstructures. Fig. 2 shows the microstructural evolution

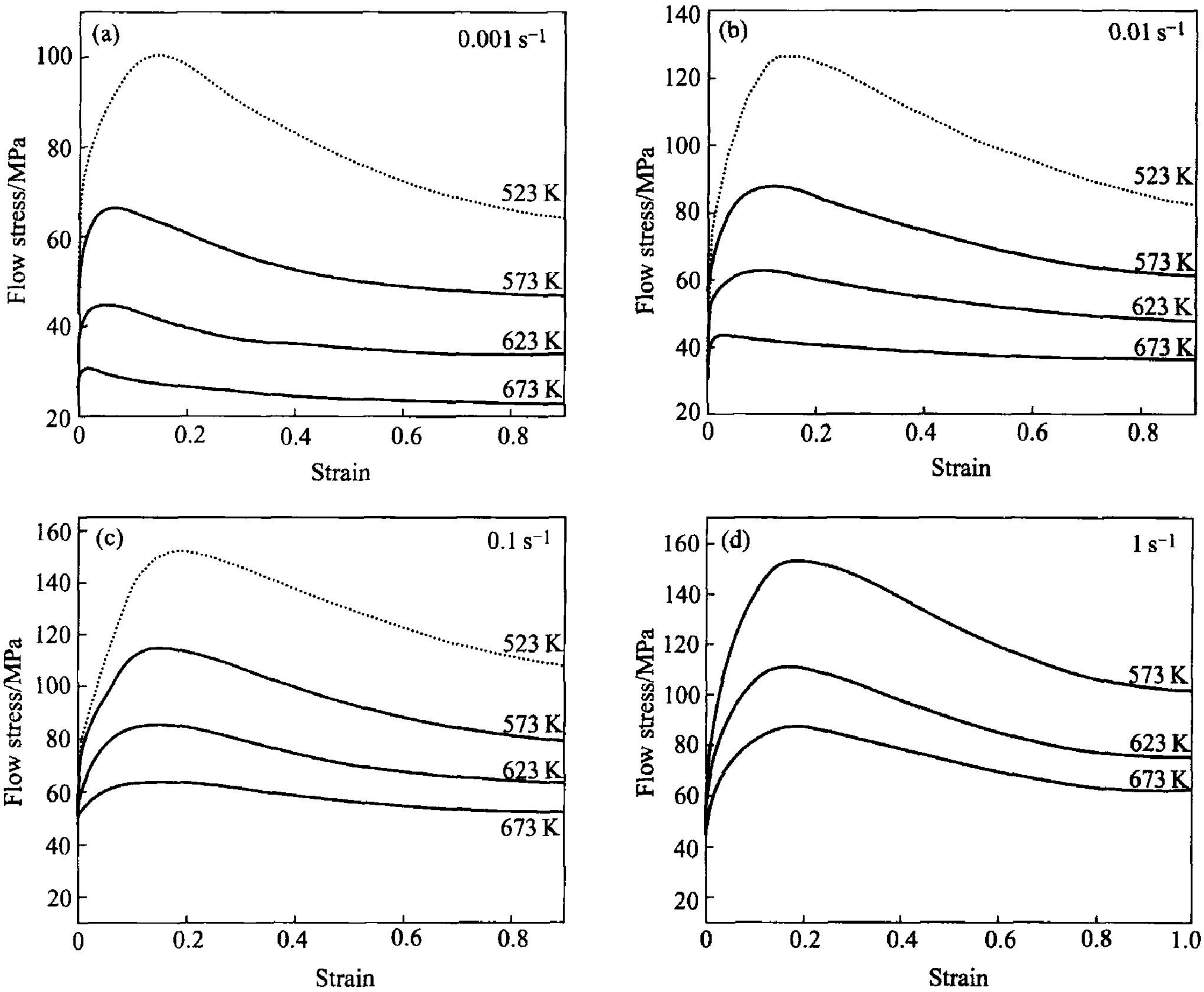


**Fig. 1** Flow stress—strain curves of AZ61 alloy in compression

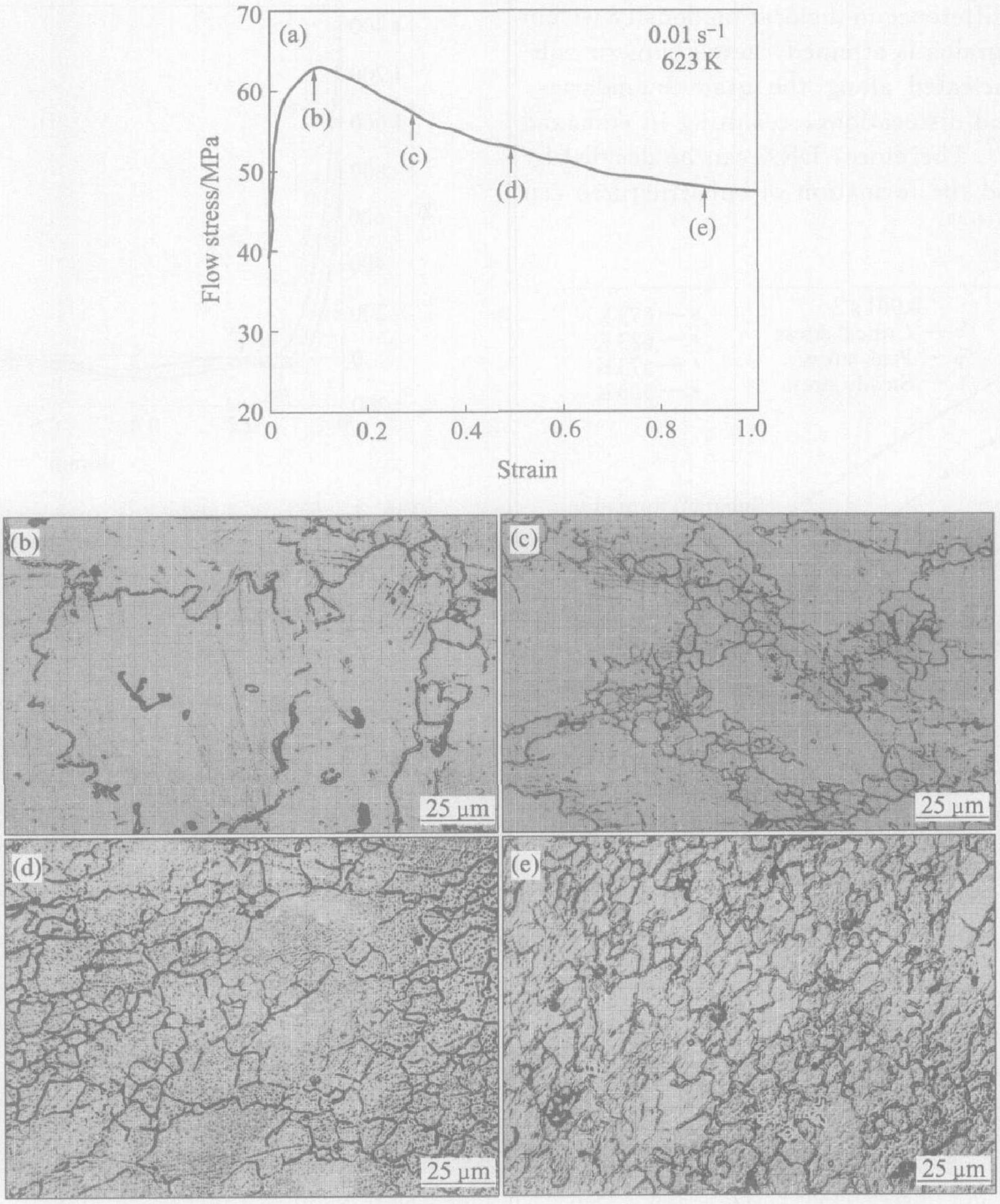


**Fig. 2** Flow stress curve and microstructures under 623 K and 0.01 $s^{-1}$
(a) —Flow stress curve; (b) —$\varepsilon$= 0.10; (c) —$\varepsilon$= 0.3; (d) —$\varepsilon$= 0.5; (e) —$\varepsilon$= 1.0

along with the strain at 623 K and strain rate of 0.01 $s^{-1}$. The microstructure of the specimen at the peak strain (0.10) is composed of both strain-hardened grains and DRX grains. When the strain is larger than the peak strain, the volume fraction of DRX increases gradually. When the strain is large enough (e.g. 1.0), only DRX grains can be observed. Especially, Figs. 2(b) and 2(c) show the recrystallized grains along the original grain boundaries.

### 3.2 $\Theta$—$\sigma$ analysis

The flow stress dependence of the strain hardening rate $\Theta(d\sigma/d\varepsilon)$ is illustrated in Fig. 3 under various conditions. The strain hardening rate decreases rapidly at the early stage of deformation. However, the decreasing rate changes with temperature and strain rate. As the temperature decreases and strain rate increases, $\Theta$ linearly increases. For instance, $\dot{\varepsilon}$= 0.001 $s^{-1}$ as the flow stress increases, the rate of decrease of $\Theta$ decelerates until the critical stress ($\sigma_c$) corresponding to the occurrence of DRX reaches, and it changes until $\Theta$ reaches zero at which the flow stress approaches its peak, and then keeps steady. It should be noted that the point at $\Theta$= 0 is just the inflection different from other alloys[11]. In most of the curves of $\Theta$, $\Theta$ is around $\Theta$−0 after the curves are the inflection point. This illustrates that strain hardening rate and strain softening rate balance each other after the peak stress. As shown in Fig. 3, the $\Theta$—$\sigma$ curves can be divided into four segments. The approximately linear segment of the $\Theta$—$\sigma$ curve is extrapolated to $\Theta$= 0 with an idealized method[14]. Based on this method, critical stress ($\sigma_c$), peak stress ($\sigma_p$) and steady stress ($\sigma_s$) can be obtained.

When the critical stress (driving force) originated from a large difference in dislocation density within subgrains or grains is attained, new grains or subgrains are nucleated along the grain boundaries, twin bands and dislocations, resulting in equiaxed DRX grains[15]. Therefore, DRX can be decided by the curve, and the formation of substructures can be predicated[14, 16].

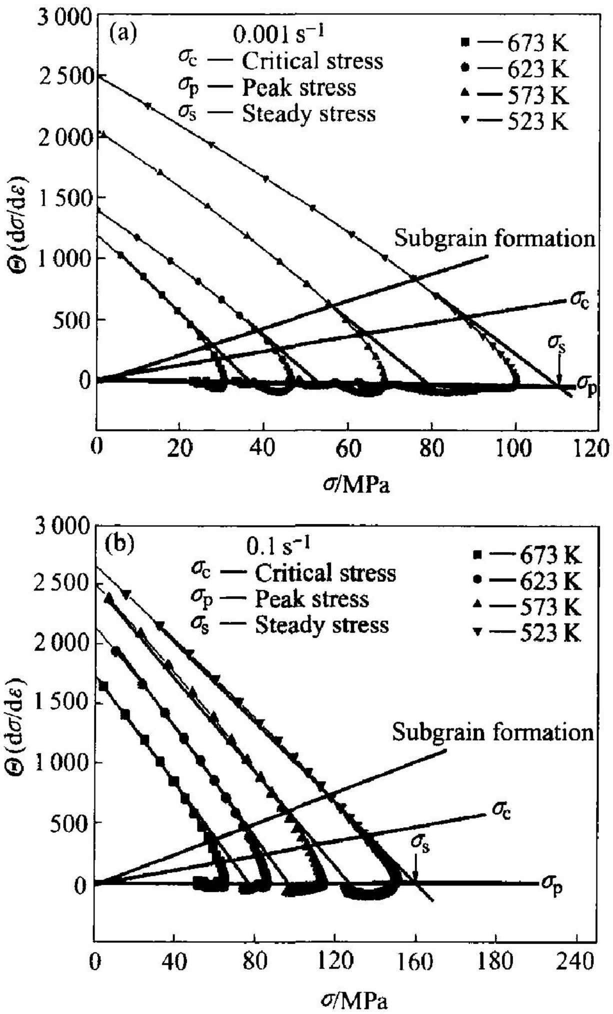


**Fig. 3** Flow stress dependence of strain-hardening rate under different conditions

(a) —$\dot{\varepsilon}$= 0.001 s$^{-1}$; (b) —$\dot{\varepsilon}$= 0.1 s$^{-1}$

Fig. 4 shows the analysis of $\Theta$—$\sigma$ curves under various deformation conditions. These curves indicate the evolution of DRX with strain. The strain that corresponds to the maximum softening rate ($\varepsilon_m$) increases with increasing strain rate or decreasing temperature. From such a curve, the onset and finish of DRX, i. e. the peak strain ($\varepsilon_p$) and the strain for maximum softening rate ($\varepsilon_m$) can be decided[14, 16]. The negative value of $\Theta$ means that softening is progressed against $\varepsilon$. Therefore, a minimum value of $\Theta$ corresponds to the maximum softening rate, after which the evolution of DRX over the strain slowly decreases and then approaches to the steady state.

Based on the analysis of $\sigma$—$\varepsilon$, $\Theta$—$\sigma$ and $\Theta$—$\varepsilon$, Eqs. (1)−(3) can be obtained through linear regression as shown in Figs. 5 and 6.

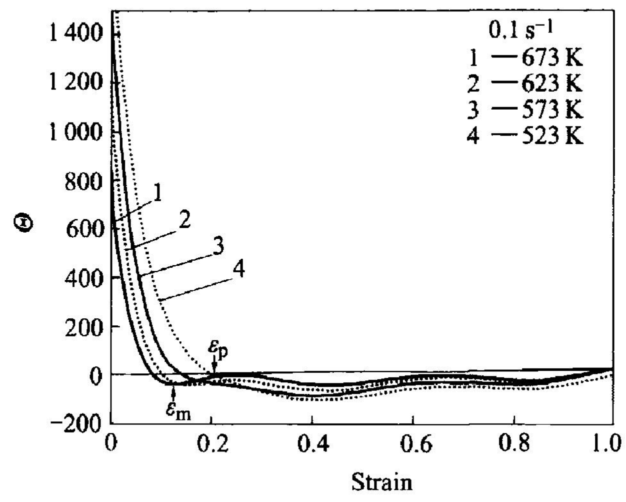


**Fig. 4** Strain hardening rate—strain curves

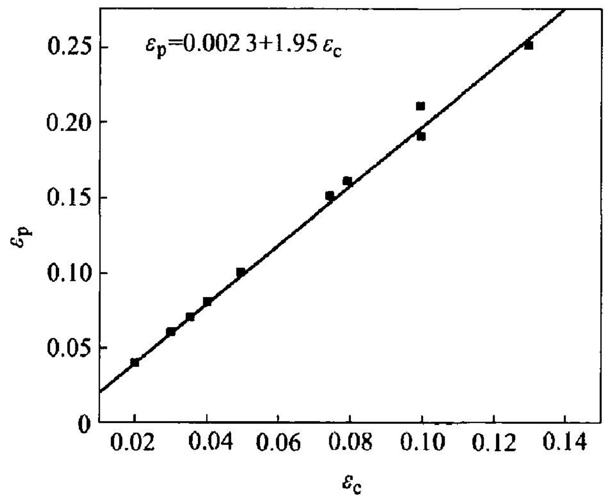


**Fig. 5** Relationship between $\varepsilon_c$ and $\varepsilon_p$

$$\varepsilon_p = 0.002\,3 + 1.95\varepsilon_c \tag{1}$$

$$\ln \varepsilon_p = -5.97 + 0.110 \ln Z \tag{2}$$

$$\ln \varepsilon_m = -4.796 + 0.088 \ln Z \tag{3}$$

where $Z$ is the Zener-Hollomon parameter ($Z = \dot{\varepsilon}\exp(185/RT)$)[17]. This suggests that $\varepsilon_p$ and $\varepsilon_m$ have a linear relationship with $\ln Z$.

Because the first item on the right of Eqn. (1) is very small (0.002 3), Eqn. (1) can be simplified as $\varepsilon_p = 1.95\varepsilon_c$. Thus,

$$\varepsilon_c \approx 0.5\varepsilon_p \tag{4}$$

Apparently, Eqn. (4) is different from the formula $\varepsilon_c = 0.6-0.8\varepsilon_p$ for micro-alloyed steel[18], indicating that the initiation of DRX of magnesium alloy is easier than that of micro-alloyed steel.

From Eqns. (2) and (4), $\varepsilon_c$ can also be assumed to have a linear relationship with $\ln Z$. Thus, $\varepsilon_c$, $\varepsilon_p$ and $\varepsilon_m$ are all linearly related to $\ln Z$.

$$\ln \varepsilon_c = 6.80 + 0.11 \ln Z \tag{5}$$

## 3.3 Predication of recrystallized volume fraction

During hot deformation, grain refinement is achieved by DRX that generally occurs at grain

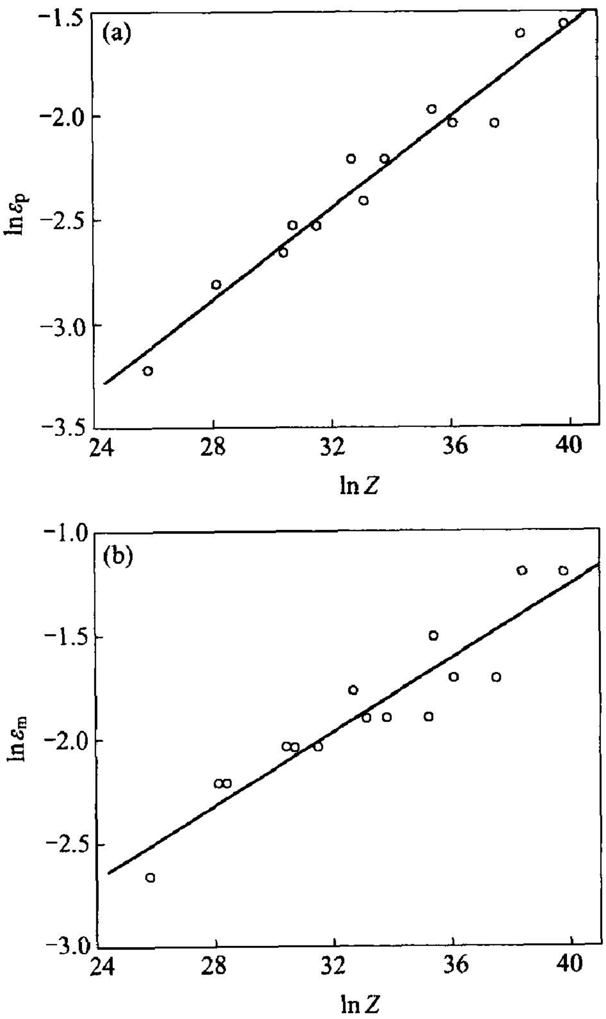


**Fig. 6** Dependence of $\varepsilon_p$ and $\varepsilon_m$ on $\ln Z$

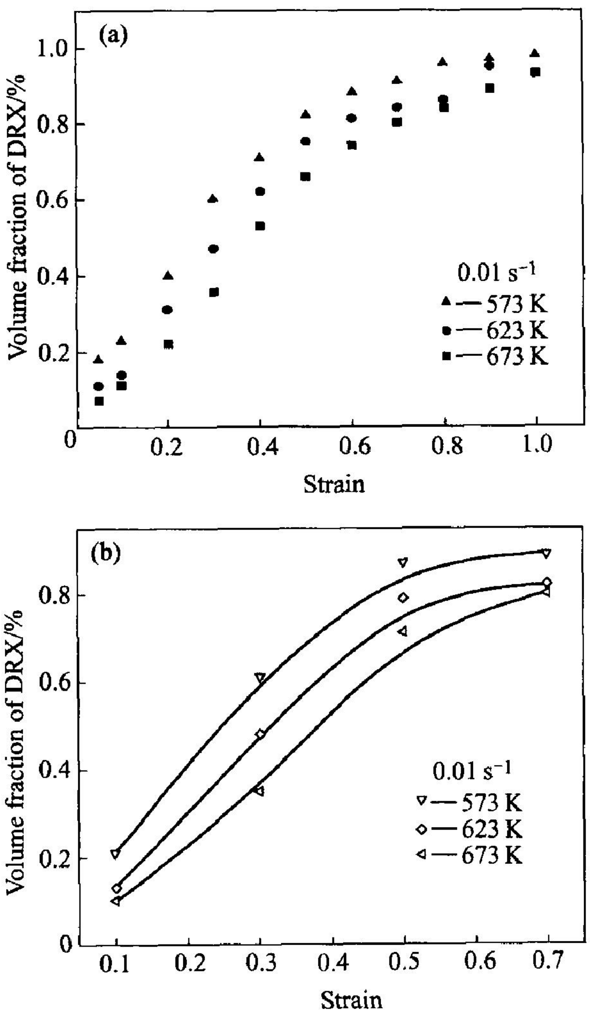


**Fig. 7** $\varphi_d$ under various deformation conditions
(a) —Predicated by Eqn. (6);
(b) —Calculated by flow curves

*boundaries and deformation bands. Microstructure observations suggest that DRX grains are almost equally sized and equiaxed, as shown in Fig. 2.*

However, the volume fraction ($\varphi_d$) of DRX is changed with deformation conditions. Generally, the kinetics of DRX can be described by an Avrami's equation under continuous recrystallization[9, 19]. Because magnesium alloy can create continuous recrystallization, the volume fraction of DRX grains during high temperature deformation can be predicated.

$$\varphi_d = 1-\exp[-k((\varepsilon-\varepsilon_c)/\varepsilon_p)^m] \quad (6)$$

where $k$, $m$ are Avrami constants respectively. Using experiment data and nonlinear regression, the following formula can be obtained.

$$\varphi_d = 1-\exp[-0.26((\varepsilon-\varepsilon_c)/\varepsilon_p)^{1.05}] \quad (7)$$

Since $\varepsilon_p$ and $\varepsilon_m$ are functions of the $Z$-parameter, $\varphi_d$ is also a function of $Z$-parameter. This suggests that $\varphi_d$ should vary with temperature, strain and strain rate. Fig. 7(a) shows the predicated volume fraction of DRX with Eqn. (7) under various conditions. Fig. 7(b) shows the calculated $\varphi_d$ under various deformation conditions based on the method of flow curves[20]. Compared with Figs. 7(a) and (b), it is found that the predicated results agree with the calculated results based on flow curves. All the $\varphi_d$ curves display S shape.

### 3.4 Microstructure and grain size of DRX

Fig. 8 shows the evolution of microstructures at the strain rate of 0.01 s$^{-1}$ and various temperatures with strain of 1.0. As shown in Fig. 8(a) and (b), at 523 − 573 K, the grains are broken and elongated. DRX occurs partially and the grain distribution is heterogeneous. Most recrystallized sites are composed of necklace structure, which is strongly dependent on the crystallographic orientation of the grain. Since gradients near the grain boundaries provided potential nucleation site for DRX[21], DRX generally initiates at grain boundaries and finally replaces original grains[22]. Above 573 K, DRX finishes completely, and the DRX grains have a homogeneous distribution. The new grains completely replaces the original grains with features of equiaxed grains. When the average size of DRX grains ($d$) in each image is plotted with the logarithm value of corresponding $Z$ as the horizontal axis, Fig. 9 is obtained. As the plot shows,

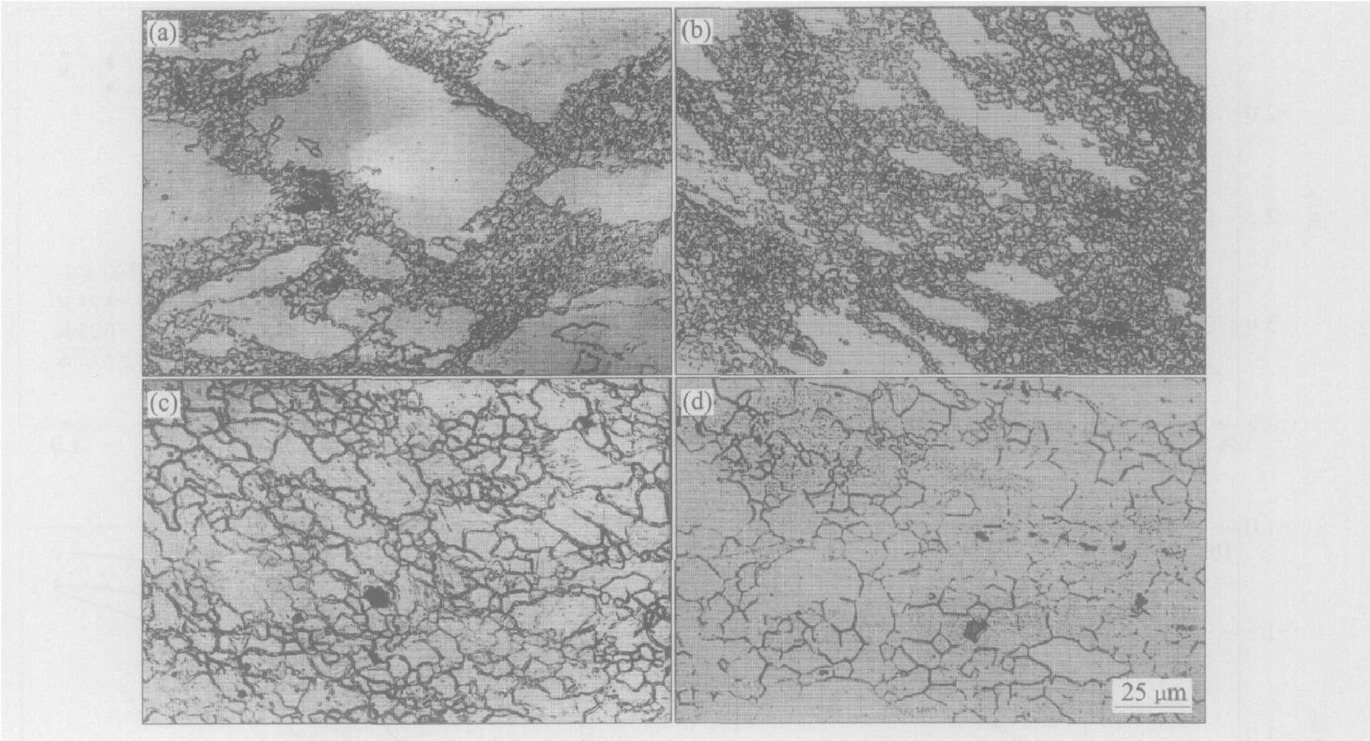


**Fig. 8** Micrographs of AZ61 alloy with strain rate $1\times10^{-2}s^{-1}$
(a) —523 K; (b) —573 K; (c) —623 K; (d) —673 K

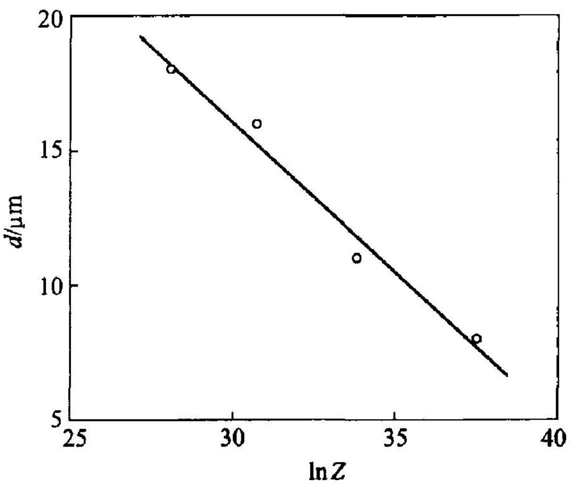


**Fig. 9** Relation between grain size and Zener-Hollomon parameter

$d$ can be formulated as a linear function of $Z$ (Eqn. (8)).

$$d = 49.56 - 1.012\ln Z \quad (8)$$

## 4 CONCLUSIONS

1) Flow softening of AZ61 alloy is found to occur at all temperatures and strain rates studied, which has a peak and a stable regime on flow curves which can be used for analyzing the initiation and evolution of DRX.

2) The critical strain($\varepsilon_c$), peak strain($\varepsilon_p$) can be defined from the analysis of flow stress curves and have a linear relationship with $\ln Z$.

3) The volume fraction of DRX ($\varphi_d$) can be described by an Avrami equation in terms of processing parameters such as strain rate($\dot{\varepsilon}$), temperature($T$), and strain($\varepsilon$), while the recrystallized grain size ($d$) can also be expressed by Zener-Hollomon parameter.

## REFERENCES

[1] Sherby O D, Nieh T G, Wadsworth J. Some thoughts on future directions for research and applications in superplasticity [J]. Materials Science Forum, 1997, 11: 243 - 245.

[2] Mukai T, Watanabe H, Higashi K. Application of superplasticity in commercial magnesium alloy for fabrication of structural components [J]. Material Science and Technology, 2000, 16(11 - 12): 1314 - 1321.

[3] Loreth M, Morton J, Jacobson K, et al. Magnesium's future in automotive components: competing for the lightweight market in North American [A]. MacEwan S, Gilardeau J P. Recent Metallurgical Advances in Light Metals [C]. Met Soc CIM, Montreal, 1995. 11 - 24.

[4] ASM Specialty Handbook. Magnesium and Magnesium Alloys [M]. Materials Park, Ohio: ASM International, 2000. 2 - 7.

[5] Closset B. Mechanical properties of extruded magnesium alloys [A]. Magnesium and Magnesium Alloys [M]. Materials Park, Ohio: ASM International, 2000. 275 - 283.

[6] Roucoules C, Yue S, Jonas J J. Effect of alloying elements on metadynamic recrystallization in HSLA steels [J]. Metall Mater Trans, 1995, A26: 181 - 189.

[7] Roucoules C, Hodgson P D, Yue S, et al. Softening and microstructural change following the dynamic recrystallization of austenite [J]. Metall Mater Trans, 1994, A25: 389 - 396.

[8] Mabuchi M, Ameyama K, Iwasaki H, et al. Low temperature superplasticity of AZ91 magnesium alloy with non-equilibrium grain boundaries[J]. Acta Mater, 1999, 47(7): 2047－2057.

[9] Ion S I, Humphrys F J, White S H. Dynamic recrystallization and the development of microstructure during the high temperature deformation of magnesium [J]. Acta Metal, 1982, 30: 1909－1919.

[10] Tan J C, Tan M J. Dynamic continuous recrystallization characteristics in two stage deformation of Mg-3Al-1Zn alloy sheet [J]. Mater Sci and Eng, 2003, A339: 124－132.

[11] Galiyev A, Kaibyshev R, Gottstein G. Correlation of plastic deformation and dynamic recrystallization in magnesium alloy ZK60 [J]. Acta Metall, 2001, 49: 1199－1207.

[12] Sakai T, Jonas J J. Dynamic recrystallization: mechanical and microstructural considerations [J]. Acta Metal, 1984, 32: 189－198.

[13] Humphreys F J. Network model for recovery and recrystallization [J]. Script Mater, 1992, 27(1): 1557－1565.

[14] Ryan N D, McQueen H J. Dynamic softening mechanisms in 304 austenitic stainless steel [J]. Can Metal Q, 1990, 29: 147－155.

[15] Mwembela A, Konopleva E, McQueen H J. Microstructural development in Mg alloy AZ31 during hot working [J]. Scripta Mater, 1997, 37: 1789－1795.

[16] Ryan N D, McQueen H J, Evangelista E. Dynamic recovery and strain hardening in the hot deformation of type 317 stainless steel [A]. Hansen N, et al. Metallurgy and Materials Science [M]. National Laboratory, Roskilde, Denmark, 1986. 527－534.

[17] Zhou H T, Zeng X Q, Ma C J, et al. A flow stress model for AZ61 alloy [J]. Acta Metallurgica Sinica, 2004, 17: 155－160.

[18] Ko B C, Yoo Y C. Hot-deformation behaviour of AA2124 composites reinforced with both particles and whiskers of SiC [J]. Mater Sci Technol, 1998, 58: 479－488.

[19] Luton M J, Sellars C M. Dynamic recrystallization in nickel and nickel-iron alloys during high-temperature deformation [J]. Acta Metall, 1969, 17: 1033－1041.

[20] Mo W M, Zhao X B. Dynamic recrystallization [A]. Recrystallization and Grain Growth [M]. Beijing: Metallurgical Industry Press, 1994. 345. (in Chinese)

[21] Kaibyshev R O, Solokov B K. Influence of crystallographic texture on slip and dynamic recrystallization of magnesium alloys[J]. Phys Met Metall, 1992, 741: 72－80.

[22] Kaibyshev R O, Sitditkov O S. Structural changes during plastic deformation of pure magnesium[J]. Phys Met Metall, 1992, 736: 635－642.

**(Edited by YUAN Sai-qian)**